Efficient porous carbon-supported MgO catalysts for the transesterification of dimethyl carbonate with diethyl carbonate

Guoming Zhao [a,b], Jinghui Shi [a], Gang Liu [a,*], Yan Liu [a], Zhenlu Wang [a], Wenxiang Zhang [a], Mingjun Jia [a,*]

[a] State Key Laboratory of Theoretical and Computational Chemistry, College of Chemistry, Jilin University, Changchun 130023, China
[b] Key Laboratory of Biofuels, Qingdao Institute of Bioenergy and Bioprocess Technology, Chinese Academy of Sciences, Qingdao 266101, China

ARTICLE INFO

ABSTRACT

Well-dispersed carbon-supported MgO catalysts were prepared using a kind of porous carbon (NC-2) as support and magnesium nitrate solution as MgO precursor by a simple wet impregnation technique. Various characterization techniques, including XRD, N2 sorption, DRIFT, XPS and TPD, were carried out to investigate their physical–chemical properties, the states of MgO species and the interaction between MgO and NC-2 materials. The catalytic properties of MgO/NC-2 catalysts were investigated in the liquid-phase transesterification of dimethyl carbonate (DMC) with diethyl carbonate (DEC). Compared with other kinds of carbon-supported MgO catalysts, MgO/NC-2 shows remarkably higher activity for the formation of ethyl methyl carbonate (EMC). Moreover, the NC-2 supported catalyst possesses very high stability against leaching of active species under test reaction conditions, indicating the truly heterogeneous nature of this catalyst. The presence of relatively rich oxygen-containing surface groups on the NC-2 carbon support should be in favor of the high dispersion of MgO particles, thus being beneficial to the fabrication of active and stable heterogeneous catalysts for the transesterificaiton reaction.

1. Introduction

As a typical solid base, magnesium oxide (MgO) has been widely used as active catalyst or catalyst support in a variety of organic reactions, such as transesterification [1], dehydrogenation of alcohol [2], aldol condensation [3–6], isomerization of alkenes [7,8], and cycloaddition of CO_2 to epoxides [9].

Conventionally, MgO catalysts could be easily obtained by the thermal decomposition of magnesium hydroxide or carbonate [10]. However, the resultant MgO catalysts usually exhibit some disadvantageous, like small specific surface areas, inhomogeneous morphologies, and varied grain size, which are considerably limited their application [11]. Hence, much effort has been devoted to synthesize novel MgO-based materials with desirable characteristics (e.g., high specific surface area, nanostructure and/or mesoporous porosity). For instance, nanoscale MgO materials with high specific surface area have been synthesized by sol–gel methods combining a hypercritical drying procedure [12–15]. MgO cubes with controllable particle size could be obtained by chemical vapor deposition method [16]. However, these approaches appear to be rather expensive and complex for conventional catalytic applications. Furthermore, mechanical strength of MgO itself is rather low,

and shaping these materials to strong catalyst particles is cumbersome. Taking these aspects into account, it is still an interesting subject to develop simple and efficient method for synthesizing MgO-based materials with advantage features.

In a work reported by Zhu and co-workers, they found that MgO-coated mesoporous SBA-15 material with relatively strong basicity could be synthesized by direct adding magnesium acetate into the initial mixture for the synthesis of mesoporous SBA-15 [17]. This result suggested that MgO supported materials with desirable characteristics may be obtained by selecting suitable support and synthesis strategy. Compared with conventional supports of silica and alumina, carbon is another kind of important support for the preparation of supported catalysts. In general, carbon structure is resistant to acidic or basic media, and the interaction between carbon and active phase is weak and the behavior of the catalyst will basically governed by the chemical nature of the active phase [18]. Recently, the rapid development in the synthesis of nanostructured carbon materials (e.g., mesoporous carbon, carbon nanofibers, carbon nanotubes) provides numerous opportunities for the preparation of novel supported metal and metal oxide catalysts [19–21]. For example, bimetallic Pt–Ru nanoparticles supported mesoporous carbon, in which the carbon support were synthesized using mesoporous SBA-15 as the hard template, exhibited excellent electrocatalytic performance and long-term durability for the application in direct methanol fuel cell [22]. Mg–Al hydrotalcites were precipitated in the porous carbon bodies

* Corresponding authors. Tel.: +86 431 85155390; fax: +86 431 8499140.
E-mail addresses: lgang@jlu.edu.cn (G. Liu), jiamj@jlu.edu.cn (M. Jia).

by consecutive impregnation of the reactants and an aging step, and exhibited very high catalytic activity for the condensation reaction [23,24].

Very recently, our groups reported a simple and efficient route for the synthesis of porous carbon (denoted as NC-2) with mesoporous and/or microporous characteristics by carbonizing a kind of composite (CA-SU/AlPO) containing citric acid (CA), sucrose (SU) and aluminum phosphate [25]. We found this material possesses abundant surface oxygen-functional groups and could be directly used as active and recyclable catalysts for the aerobic oxidation of benzyl alcohol [26].

Herein, we attempted to fabricate carbon-supported MgO nanocomposites using NC-2 carbon material as support and magnesium nitrate as MgO precursor through a wet impregnation method. The catalytic properties of these materials were investigated in the liquid-phase transesterification of dimethyl carbonate (DMC) with diethyl carbonate (DEC), which is an important base-catalytic reaction for the synthesis of ethyl methyl carbonate (EMC, an important cosolvent in a nonaqueous electrolyte) [27–29]. Previously, it was reported that solid base of MgO is one of the most active catalysts for this reaction [30]. In the present work, we found that the resultant MgO/NC-2 catalysts exhibit remarkably higher transesterification activity than other carbon-supported MgO catalysts. Combining a variety of characterization results, the catalytic property of MgO/NC-2 was correlated with the surface chemistry of the carbon materials.

2. Experimental

2.1. Catalysts preparation

Porous carbon (NC-2) support was prepared by direct carbonizing a composite (CA-SU/AlPO) containing citric acid (CA) and aluminum phosphate as reported previously [25]. Typically, H_3PO_4 (85 wt.%) was dropped into a mixed aqueous solution of $Al(NO_3)_3 \cdot 9H_2O$, sucrose (SU) and CA under vigorous stirring at ambient temperature, leading to a composition in molar ratio of SU/CA/P/Al = 1.0/0.5/1.0/1.0. Then an aqueous ammonia solution (10 wt.%) was used to adjust the pH value of the solution to 5.0. The solid CA-SU/AlPO composite was formed after removing water and all other volatiles by heating the mixed solution at 363 K for 10 h. After that, the CA-SU/AlPO composite was pretreated at 573 K in open air for a few minutes, then carbonization of the composite was carried out at 1073 K for 6 h under an argon flow. The black carbonized composite was treated with 4 M HNO_3 solution at 323 K to remove AlPO component, and is filtered and dried at 383 K to obtain the resulting NC-2 carbon materials. Moreover, an additional method was used to modify the surface chemistry of the NC-2 carbon material: heat-treatment at 1073 K in the flow of H_2 for 6 h to obtain a modified NC-2 material (denoted as NC-2 (H_2)). Except for special mention, the carbon material is referred to the one that is not modified.

Reference samples of SBA-15 and CMK-3 were prepared according to a literature procedure [19]. Commercially available coal-based activated carbon (denoted as CC, from Ningxia Henghui Actived Carbon Co. Ltd.) and almond nutshells-based activated carbon (denoted as AC, from Limin Active Carbon Co. Ltd.) were also used in this study.

The carbon-supported MgO catalysts were synthesized by wet impregnation method. Typically, a fully dried carbon support was added into a water solution of $Mg(NO_3)_2$, and the resultant mixture was stirred for about 3 h to impregnate the activated carbon with Mg-containing solution at room temperature. After that, water was evaporated away from the mixture at a temperature of 353 K under atmosphere pressure. The resultant solid composite was calcined at 1073 K for 6 h under an argon flow. The loading of MgO was in the range of 1.6–20.0 wt.%.

For comparison, SBA-15 supported MgO catalyst (with 4.0 wt.% MgO loading) was prepared using the above procedure. To have basic sites exposed on the surface, pretreatment at relatively high temperature was required under inert atmosphere [31]. The catalyst was calcined at 1073 K for 2 h in argon before it was used in the transesterification reaction.

2.2. Catalytic performance

The typical liquid-phase transesterification of DMC with DEC was carried out as follows: 4.5 g (0.05 mol) of dimethyl carbonate, 5.9 g (0.05 mol) of diethyl carbonate and 0.5 g of the catalyst were charged to a 50-mL one-neck flask. Then the mixture was heated up to 376 K with stirring under N_2 atmosphere to start the reaction. The reaction products were analyzed by a gas chromatography (GC-8A) equipped with an HP-5 capillary column and FID.

2.3. Characterization

N_2 adsorption/desorption isotherms were measured at 77 K, using a Micromeritics ASAP 2010N analyzer. Samples were degassed at 523 K for 8 h before measurements. Specific surface areas were calculated using the BET model. Pore volumes were estimated at a relative pressure of 0.94 (P/P_0), assuming full surface saturation with nitrogen. Pore size distributions were evaluated from desorption branches of nitrogen isotherms using the BJH model.

Powder XRD diffraction patterns were recorded on Shimadzu XRD-6000 diffractometer (40 kV, 30 mA) using Ni-filtered Cu Kα radiation.

DRIFT spectra were recorded on a Nicolet AVATAR 370 DTGS spectrometer. After drying in air at 393 K, the carbon samples were mounted on the sample holder of the DRIFT attachment. The DRIFT spectrum of each sample was recorded from 256 scans at a resolution of 2 cm^{-1}.

The temperature-programmed desorption of carbon dioxide (CO_2-TPD) was carried out on Autochem II 2920 (Micromeritics, USA). The sample (100 mg) was first placed in the reactor and treated at 1073 K for 2 h in air. After cooling to 323 K, the sample was exposed to 10% CO_2/Ar mixture flow (20 ml/min) for 1 h. Then the sample was flushed in Ar flow at 323 K for removal of physically adsorbed CO_2. An CO_2-TPD profile of the sample was recorded by increasing the temperature from 323 to 1073 K at a heating rate of 10 K/min under 20 mL/min of Ar flow. The desorbed products were analyzed by a quadrupole mass spectrometer (FISONS Instruments). The concentrations of CO_2 were determined by the intensities of m/z at 44.

3. Results and discussion

3.1. Catalyst characterization

Fig. 1 shows the XRD patterns of different carbon supports and the supported MgO catalysts (with 4.0 wt.% MgO loading). All carbon supports exhibit two broad diffraction peaks centered at 26° and 44°, which can be generally indexed to (0 0 2), (1 0 1) diffraction for glass-like carbon bearing graphitic characteristics [25,32]. Besides, the 4.0 wt.% MgO/CMK-3 sample shows two weak diffraction peaks centered at 43° and 63°, which can be generally indexed to (2 0 0), (2 2 0) diffraction for the presence of a certain amount of MgO crystalline phase [33]. While the peaks due to MgO phase are not found in the patterns of 4.0 wt.% MgO/NC-2, 4.0 wt.% MgO/CC and 4.0 wt.% MgO/AC, indicating that MgO species should be highly dispersed on the surface of these carbon supports.
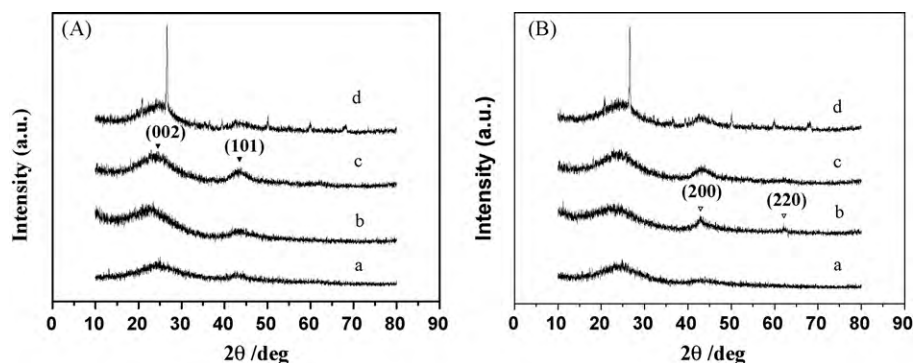
Fig. 1. (A) XRD patterns of different supports: (a) NC-2; (b) CMK-3; (c) AC; (d) CC (▼: diffraction for glass-like carbon bearing graphitic characteristics). (B) XRD patterns of the carbon-supported 4.0 wt.% MgO catalysts (▽: diffraction for the presence of a certain amount of MgO crystalline phase).
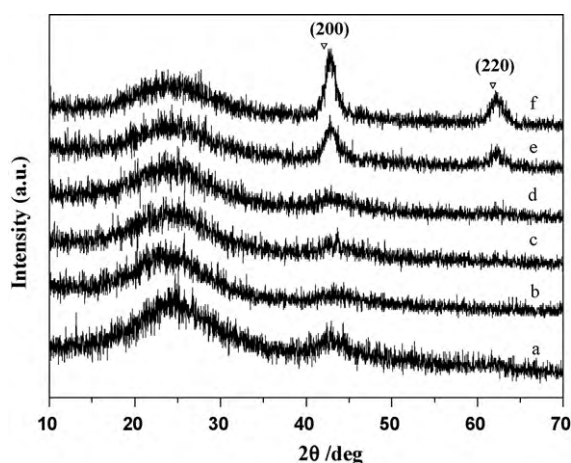

Fig. 2. XRD patterns of MgO/NC-2 catalysts with different MgO contents: (a) NC-2; (b) 1.6 wt.% MgO/NC-2; (c) 4.0 wt.% MgO/NC-2; (d) 7.7 wt.% MgO/NC-2; (e) 14.3 wt.% MgO/NC-2; (f) 20.0 wt.% MgO/NC-2 (▽: diffraction for the presence of a certain amount of MgO crystalline phase).
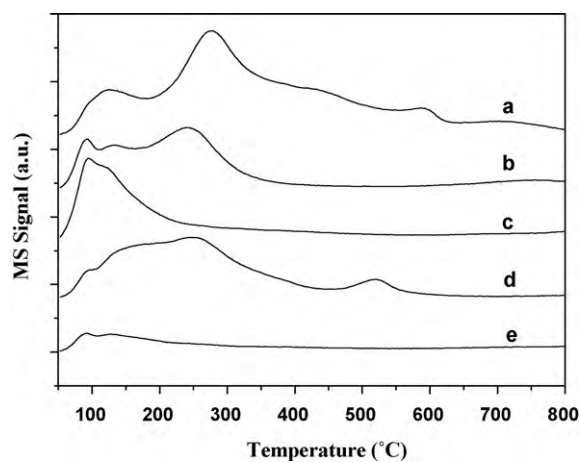

Fig. 3. CO_2-TPD profiles of the pure MgO and carbon-supported MgO catalysts: (a) 4.0 wt.% MgO/AC; (b) 4.0 wt.% MgO/CC; (c) 4.0 wt.% MgO/NC-2; (d) MgO; (e) 4.0 wt.% MgO/CMK-3.

Fig. 2 shows the XRD patterns of a few representative samples of the MgO/NC-2 composites with different Mg loading. It can be seen that MgO species could be highly dispersed on the NC-2 support even the loading of MgO reaches 7.7 wt.%. With further increasing the MgO loading (equal or above 14.3 wt.% MgO), significant MgO crystalline phase can be observed.

The relevant structure parameters of the carbon-supported MgO samples and their parent carbon supports are given in Table 1. Compared with the carbon supports, the corresponding carbon-supported MgO samples show lower specific surface area, smaller pore volume and mean pore size, which can be assigned to the deposit of magnesium oxides on the walls and/or in the mouth of the smaller pores of the carbon materials.

The basicity of the supported MgO/NC-2 catalysts was investigated by CO_2-TPD (Fig. 3). Pure MgO shows a very broad CO_2 desorption peak, extended from 353 to 823 K, which could be assigned to the existence of weak and medium basic sites, associated to the Mg^{2+}–O^{2-} pairs. The presence of a certain amount of weak and medium basic sites could be also observed on the samples of 4.0 wt.% MgO/CC and 4.0 wt.% MgO/AC. The area of desorption peak of 4.0 wt.% MgO/CMK-3 is much less than other three carbon-supported MgO catalysts, indicating that the number of basic sites is quite low in this sample. This might be mainly due to the fact that MgO species exist in the form of large crystalline particles over the sample of MgO/CMK-3 as suggested by the XRD characterization. Notably, the desorption peak of 4.0 wt.% MgO/NC-2 turns to narrow, implying that MgO species should be uniformly dispersed on the surface of NC-2. Compared with pure MgO and other carbon-supported MgO catalysts, the basicity of MgO/NC-2 decreases somewhat, which should be caused by the presence of relatively strong interaction between MgO species and NC-2 support. It should be mentioned here that there are nearly no detectable basic sites on the surface of MgO/SBA-15 (not shown).

Table 1
The structure parameters of carbon supports and carbon-supported MgO catalysts.

Samples	BET surface area ($m^2 g^{-1}$)	Pore vol. ($cm^3 g^{-1}$)	Pore size[a] (nm)
NC-2	1072	0.91	3.5
4.0 wt.% MgO/NC-2	797	0.70	3.3
CMK-3	1564	1.51	4.0
4.0 wt.% MgO/CMK-3	1453	1.27	3.4
4.0 wt.% MgO/AC	779	0.13	3.2
4.0 wt.% MgO/CC	862	0.28	2.6

[a] Calculated using the BJH model on the desorption branch of the N_2 adsorption/desorption isotherms.
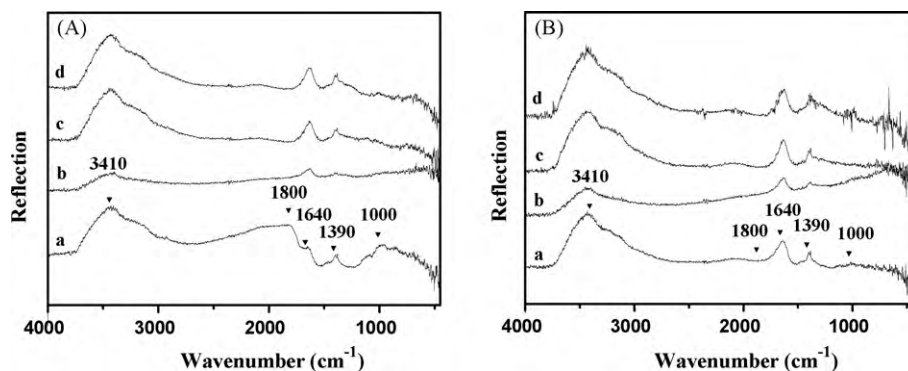
Fig. 4. (A) DRIFT spectra of different carbon supports: (a) NC-2; (b) CMK-3; (c) AC; (d) CC. (B) DRIFT spectra of the carbon-supported 4.0 wt.% MgO catalysts: (a) MgO/NC-2; (b) MgO/CMK-3; (c) MgO/AC; (d) MgO/CC.

This might be due to the fact that the abundant hydroxyl groups (Si–OH) existed on the surface of SBA-15 could easily react with MgO species to form inactive magnesium silicate species under the preparation conditions.

Fig. 4 shows the DRIFT spectra of different carbon supports and the supported 4.0 wt.% MgO catalysts. The broad bands centered at 1390 and 1000 cm^{-1} can be mainly assigned to the C–O stretch vibrations in ether type structure [26]. The broad band in 3100–3500 cm^{-1} region can be attributed to the O–H stretch vibrations from hydroxyl, phenolic and carboxylic groups [26]. The appearance of very broad bands in the range of 1600–2300 cm^{-1} can be attributed to the stretching vibrations of C=O moieties in (i) quinone or conjugated ketone structure (around 1640 cm^{-1}); (ii) carboxylic acid, lactone, acid anhydride (in the range of 1670–1900 cm^{-1}) [26,34–36]. Among these carbon supports, it can be seen that NC-2 possesses relatively abundant surface oxygen-functional groups. After supporting MgO to the surface of carbon supports, no obvious change could be observed in the DRIFT spectra of 4.0 wt.%MgO/CMK-3, 4.0 wt.%MgO/AC and 4.0 wt.%MgO/CC in comparison with the corresponding carbon supports. However, the relative intensity of the DRIFT peaks of 4.0 wt.%MgO/NC-2 is much lower than the support of NC-2, implying that quite amount of surface oxygen-functional groups in NC-2 may interact with MgO species during the preparation process. Previously, it was reported that magnesium oxide/hydroxide could be uniformly deposited on the surface of pre-oxidized pitch-based activated carbon fibers, due to the interaction between Mg species and surface oxygen-functional groups (e.g., –COOH groups) of the carbon support [37,38]. In the present work, we suppose that the existence of abundant surface oxygen-functional groups in NC-2 may be useful for building a suitable interaction between NC-2 support and the Mg species (i.e. magnesium nitrate) during the preparation process, thus resulting in the uniform dispersion of MgO species on the surface of NC-2 support.

3.2. Catalytic performances

Fig. 5 presents the catalytic performance of various carbon-supported MgO catalysts (with 4.0 wt.% MgO loading) for the transesterification of DMC and DEC. All the catalysts are active for the transesterificaiton reaction with nearly 100% selectivity to EMC. Among them, 4.0 wt.% MgO/NC exhibits the highest activity, a 49.3% yield of EMC could be achieved after 0.5 h reaction. The catalytic activity decreases in the order: MgO/NC-2 > MgO/CC > MgO/AC > MgO/CMK-3. For comparison, the catalytic property of SBA-15 supported MgO (4.0 wt.% MgO/SBA-15) was also investigated. Very low EMC yield (0.9%) was achieved after 2 h of reaction on the MgO/SBA-15 catalyst, which is consistent to its weak basic characteristic as mentioned above. These results sug-
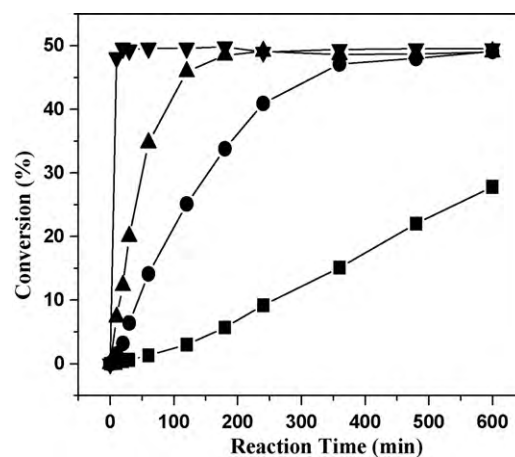
gest that carbon is an efficient support for the preparation of active MgO supported catalyst.

Fig. 6 presents the comparative results of catalytic activities of MgO/NC-2 catalysts with different Mg loading. It can be seen that the conversion of DEC increases when the MgO loading increases from 1.6 to 7.7 wt.%. With further increasing the MgO loading (up to 14.3 wt.%), the time that reaction reaches equilibrium turns to
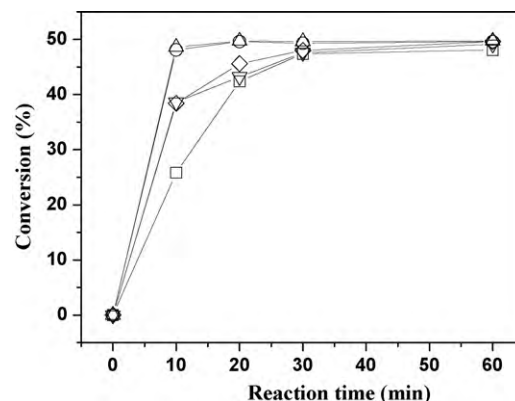

Fig. 5. Dependence of the DEC conversion on the reaction time of the carbon-supported MgO catalysts: (■) 4.0 wt.% MgO/CMK-3; (●) 4.0 wt.% MgO/AC; (▲) 4.0 wt.% MgO/CC; (▼) 4.0 wt.% MgO/NC-2; Reaction conditions: catalyst, 0.5 g; DMC, 0.05 mol; DEC, 0.05 mol; reaction temperature, 376 K.

Fig. 6. Dependence of the DEC conversion on the reaction time of the MgO/NC-2 catalyst with different MgO contents: (□) 1.6 wt.% MgO/NC-2; (○) 4.0 wt.% MgO/NC-2; (△) 7.7 wt.% MgO/NC-2; (▽) 14.3 wt.% MgO/NC-2; (◇) 20.0 wt.% MgO/NC-2 calcined at 1073 K. Reaction conditions: catalyst, 0.5 g; DMC, 0.05 mol; DEC, 0.05 mol; reaction temperature, 376 K.
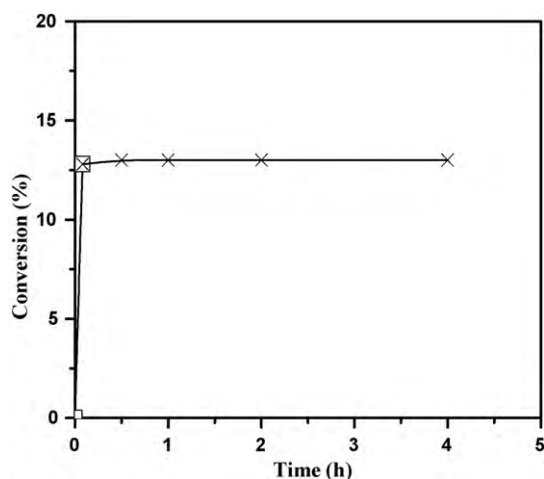
Fig. 7. Heterogeneous reaction check for 4.0 wt.% MgO/NC-2 calcined at 1073 K (□), by continuing the reaction after removing the 4.0 wt.% MgO/NC-2 catalyst (×) by filtration at reaction temperature. *Reaction conditions*: the suspension, which contained 0.05 mol of DMC, 0.05 mol of DEC and 0.5 g of catalyst, was stirred and heated to reflux temperature (376 K).

slight longer, indicating the decrease in catalytic activity of these catalysts. According to the results of XRD characterizations, it was known that MgO could be highly dispersed on the surface of NC-2 support when the loading of MgO below 14.3 wt.%. Hence, the relatively high activity of the sample with lower MgO loading (≤7.7 wt.%) may suggest that the highly dispersed MgO particles (nanoparticles) should be the main active centers for the transesterification reaction. The slight decrease in catalytic activity of the samples with higher MgO loading (≥14.3 wt.%) should be mainly assigned to the appearance of relative large crystalline MgO.

The most interesting result is the high stability of the MgO/NC-2 catalysts against leaching of the active species into the liquid phase under the given reaction conditions. In a duplicate reaction over 4.0 wt.% MgO/NC-2 (calcined at 1073 K), it was found that no detectable subsequent conversion in the solution after removing the catalyst by hot filtration at the reaction temperature (Fig. 7). This is a very strong evidence for a real heterogeneous catalysis. Moreover, it was found that MgO/NC-2 catalyst can be easily recycled (with nearly consistent activity as the fresh one) by simple heat activation of the used catalyst under an argon atmosphere at 1073 K for some while (Fig. 8).

On the basis of the characterization results of XRD, it was known that MgO species could be highly dispersed on the surface of NC-2 in
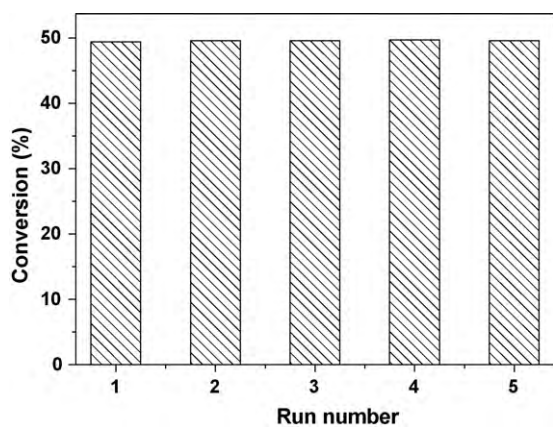

Fig. 8. Transesterification activities of 4.0 wt.% MgO/NC-2 calcined at 1073 K during five reaction cycles. *Reaction conditions*: catalyst, 0.25 g; DMC, 0.05 mol; DEC, 0.05; reaction temperature, 376 K; reaction time, 0.5 h.
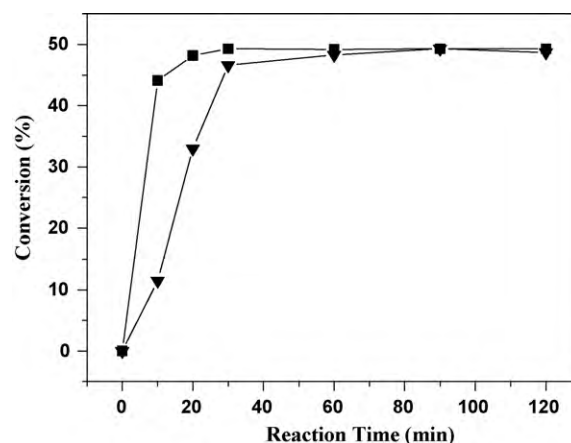

Fig. 9. Dependence of the DEC conversion on the reaction time of the 4.0 wt.% MgO/NC-2 catalyst with different supports treated method: (■) NC-2 without any disposal; (▼) NC-2 calcined at 1073 K for 6 h in the flow of H_2. *Reaction conditions*: catalyst, 0.5 g; DMC, 0.05 mol; DEC, 0.05; reaction temperature, 376 K.

the form of small MgO nanoparticles, while serious agglomeration of MgO particles on the surface of the CMK-3 occurs. This might be the main reason for why MgO/NC-2 exhibits relatively high activity compared with other carbon-supported MgO catalysts. We suppose that the structure characteristics (e.g., high specific surface area, porosity) and surface chemistry (e.g., polarity, electro-property) of NC-2 support should be beneficial to the formation of such efficient catalyst.

According to the results of DRIFT and TPD, it has been proposed that the presence of abundant surface oxygen-functional groups in NC-2 may be useful for building a suitable interaction between NC-2 support and the Mg species (i.e. magnesium nitrate) during the preparation process, thus resulting in the uniform dispersion of MgO species on the surface of NC-2 support. For the sake of a better understanding of the role of surface oxygen-functional groups, a reductive modification of the carbon materials was employed before the impregnation. In short, an additional NC-2 supported MgO catalyst (denoted as 4.0 wt.% MgO/NC-2 (H_2)) was obtained using a hydrogen-treated NC-2 as support (1073 K for 6 h in the flow of H_2). It was found from Fig. 9 that the 4.0 wt.% MgO/NC-2 (H_2) catalyst shows much lower activity than the one without additional treatment. Previously, it has been reported that most of the surface oxygen groups in carbon material could be eliminated by such hydrogen treatment [36]. Hence, the experimental results presented here confirmed further that the presence of abundant surface oxygen groups is indeed a crucial factor for the formation of highly active carbon-supported MgO catalyst. Besides, other factors, including the structure characteristics and the surface chemistry of carbon support, may also make considerable contribution to the high catalytic activity of the carbon-supported catalyst by influencing the chemisorption intensity and/or the diffusion velocity of reactants and products [39].

4. Conclusions

Well-dispersed carbon-supported MgO materials (MgO/NC-2) could be obtained using porous carbon (NC-2) as support and magnesium nitrate solution as MgO precursor through a simple wet impregnation technique. These materials are efficient heterogeneous catalysts for the liquid-phase transesterification of DMC with DEC to EMC. The presence of relatively rich oxygen-containing surface groups on the NC-2 carbon support should be in favor of the high dispersion of MgO particles, thus being beneficial to the formation of active and stable catalysts for the transesterificaiton reaction.

Acknowledgements

References

[1] M.L. Kantam, U. Pal, B. Sreedhar, B.M. Choudary, Adv. Synth. Catal. 349 (2007) 1671–1675.
[2] M.A. Aramendía, V. Borau, C. Jiménez, J.M. Marinas, A. Porras, F.J. Urbano, J. Catal. 161 (1996) 829–838.
[3] V.K. Díez, C.R. Apesteguía, J.I. Di Cosimo, J. Catal. 240 (2006) 235–244.
[4] G. Zhang, H. Hattori, K. Tanabe, Appl. Catal. 36 (1988) 189–197.
[5] J.I. Di Cosimo, V.K. Díez, C.R. Apesteguía, Appl. Catal. A: Gen. 137 (1996) 149–166.
[6] J.I. Di Cosimo, C.R. Apesteguía, J. Mol. Catal. A Chem. 130 (1998) 177–185.
[7] H. Hattori, Chem. Rev. 95 (1995) 537–558.
[8] Y. Wang, J.H. Zhu, J.M. Cao, Y. Chun, Q.H. Xu, Micropor. Mesopor. Mater. 26 (1998) 175–184.
[9] M. Tu, R.J. Davis, J. Catal. 199 (2001) 85–91.
[10] M.A. Aramendía, V. Borau, C. Jiménez, J.M. Marinas, J.R. Ruiz, F.J. Urbano, Appl. Catal. A: Gen. 244 (2003) 207–215.
[11] K.T. Ranjit, K.J. Klabunde, Chem. Mater. 17 (2005) 65–73.
[12] S. Utamapanya, K.J. Klabunde, J.R. Schlup, Chem. Mater. 3 (1991) 175–181.
[13] R.M. Richards, A.M. Volodin, A.F. Bedilo, K.J. Klabunde, Phys. Chem. Chem. Phys. 5 (2003) 4299–4305.
[14] M.E. Martin, R.M. Narske, K.J. Klabunde, Micropor. Mesopor. Mater. 83 (2005) 47–50.
[15] R. Richards, W.F. Li, S. Decker, C. Davidson, O. Koper, V. Zaikovski, A. Volodin, T. Rieker, K.J. Klabunde, J. Am. Chem. Soc. 122 (2000) 4921–4925.
[16] S. Stankic, M. Müeller, O. Diwald, M. Sterrer, E. Knözinger, J. Bernardi, Angew. Chem. Int. Ed. 44 (2005) 4917–4920.
[17] Y.L. Wei, Y.M. Wang, J.H. Zhu, Z.Y. Wu, Adv. Mater. 15 (2003) 1943–1945.
[18] F. Rodríguez-Reinoso, Carbon 36 (1998) 159–175.
[19] S. Jun, S.H. Joo, R. Ryoo, M. Kruk, M. Jaroniec, Z. Liu, T. Ohsuna, O. Terasaki, J. Am. Chem. Soc. 122 (2000) 10712–10713.
[20] M.L. Toebes, F.F. Prinsloo, J.H. Bitter, A.J. van Dillen, K.P. de Jong, J. Catal. 214 (2003) 78–87.
[21] H. Vu, F. Gonçalves, R. Philippe, E. Lamouroux, M. Corrias, Y. Kihn, D. Plee, P. Kalck, P. Serp, J. Catal. 240 (2006) 18–22.
[22] S.H. Liu, W.Y. Yu, C.H. Chen, A.Y. Lo, B.J. Hwang, S.H. Chien, S.B. Liu, Chem. Mater. 20 (2008) 1622–1628.
[23] F. Winter, V. Koot, A.J. van Dillen, J.W. Geus, K.P. de Jong, J. Catal. 236 (2005) 91–100.
[24] A. Dubey, Green Chem. 9 (2007) 424–426.
[25] G. Liu, Y. Liu, Z.L. Wang, X.Z. Liao, S.J. Wu, W.X. Zhang, M.J. Jia, Micropor. Mesopor. Mater. 116 (2008) 439–444.
[26] G. Liu, Y. Liu, X.Y. zhang, X.L. Yuan, M. Zhang, W.X. Zhang, M.J. Jia., J. Colloid Interface Sci. 342 (2010) 467–473.
[27] E.J. Plichta, W.K. Behl, J. Power Sources 88 (2000) 192–196.
[28] H. Okuno, H. Koshina, A. Morta, J. Power Sources 67 (1997) 341–1341.
[29] H. Okuno, H. Koshina, K. Hasegawa, U.S. Patent 5,484,669 (1996).
[30] Z.L. Shen, X.Z. Jiang, W.J. Zhao., Catal. Lett. 91 (2003) 63–67.
[31] H. Hattori, Appl. Catal. A: Gen. 222 (2001) 247–259.
[32] A.-H. Lu, W.-C. Li, E.-L. Salabas, B. Spliethoff, F. Schuth, Chem. Mater. 18 (2006) 2086–2094.
[33] J.C. Yu, A.W. Xu, L.Z. Zhang, R.Q. Song, L. Wu, J. Phys. Chem. B 108 (2004) 64–70.
[34] F.J. López-Garzón, M. Domingo-García, M. Pérez-Mendoza, P.M. Alvarez, V. Gómezo-Serrano, Langmuir 19 (2003) 2838–2844.
[35] S. Shin, J. Jang, S.-H. Yoon, I. Mochida, Carbon 35 (1997) 1739–1743.
[36] J.-H. Zhou, Z.-J. Sui, J. Zhu, P. Li, D. Chen, Y.-C. Dai, W.-K. Yuan., Carbon 45 (2007) 785–796.
[37] Z.-M. Wang, N. Yamashita, Z.-X. Wang, K. Hoshinoo, H. Kanoh, J. Colloid Interface Sci. 276 (2004) 143–150.
[38] Z.-M. Wang, Z.-X. Wang, N. Yamashita, K. Hoshinoo, H. Kanoh, J. Colloid Interface Sci. 276 (2004) 151–158.
[39] A. Palani, N. Gokulakrishnan, M. Palanichamy, A. Pandurangan, Appl. Catal. A: Gen. 304 (2006) 152–158.